

ANALYSIS OF ADDITION THE NUMBER OF HALF CIRCLE TYPE SLOT ON PERFORMANCE CHARACTERISTICS OF DISC CONDUCTOR EDDY CURRENT BRAKE

Alfian Jihan Saputra¹, Dominicus Danardono Dwi Prija Tjahjana^{1,2*}, Muhammad Nizam^{2,3,4}, Mufti Reza Aulia Putra¹

¹ Mechanical Engineering Department, Faculty of Engineering, Universitas Sebelas Maret, Jl. Ir. Sutami 36A, Surakarta 57126, Indonesia

² National Center of Sustainable Transportation Technology (NCSTT) ITB, Bandung 40132, Indonesia

³ Electrical Engineering Department, Faculty of Engineering, Universitas Sebelas Maret, Jl. Ir. Sutami 36A, Surakarta 57126, Indonesia

⁴ Lithium Battery Research and Technology Centre, Universitas Sebelas Maret, Jl. Slamet Riyadi 435, Surakarta 57146, Indonesia

ABSTRACT

Brake is a vital component of a vehicle, particularly for motor vehicles. One of the braking used the principle of Eddy Current Brake by utilizing electromagnetic. Eddy Current Brake is a braking technology without direct contact by utilizing eddy currents. Eddy Current Brake performance can be influenced by several factors, one of them is the surface shape of the disc conductor. Using finite element simulation, this research examines the impact of increasing the number of slot half-circles on the performance of the Eddy Current Brake with the number of slot changes. Variations number of slots that used are 6, 8, 10, and 12 slots. The result of this study obtained the best braking torque value in the variation with the number of 10 slots at a rotational speed of 450 rpm with a 15,930 Nm torque value. The addition slots of the number of half-circle types have a less significant effect on the torque from the simulation.

KEYWORDS: *Eddy Current Brake, Finite Element Method, Half-circle slotted*

1.0 INTRODUCTION

Vehicles currently use a lot of conventional brakes to slow down the speed and the most common types of brakes are drum brakes and disc brakes. In the operation of both types of brakes, the friction concept is applied. Friction that occur will change from kinetic energy to heat energy when the brake operating (Günay et al., 2020). The vehicle's speed will be reduced by friction until it comes to a halt. However, the friction between the two objects will almost definitely produce an increase in temperature surrounding the brakes (Gerdes & Hedrick, 1999).

To solve the problems developed technology on braking. Using an Eddy Current Brake (ECB) is one of them (Mufti Reza Aulia Putra et al., 2020). Eddy current brakes are

*Corresponding author. Email: ddanardono@staff.uns.ac.id

intended to be used in place of konventional brakes (Cho, Liu, Lee, et al., 2017). Karakoc also used the FEM method to analyze the dispersion of eddy currents. In his research, it was found that ECB braking can be used to replace conventional brakes (Karakoc et al., 2016). Eddy Current Braking is a sort of electric braking that relies on eddy currents for braking (Lequesne, 1997). The ECB braking system is frictionless braking which has advantages such as not producing wear, making little noise, and having a fast response (Cho, Liu, Ahn, et al., 2017). ECB is now being developed for light vehicles, such as motorcycles, in addition to being employed in large vehicles (Sinmaz et al., 2016).

In the development of ECB braking, Robert, et al. analyze the surface design of disk conductors by adding slots. The slot can be defined as a hollow shape on the surface of the disc that serves to improve braking performance. The addition of the number of slots in this study affects the resulting braking torque. The results indicated that the brake with a slotted disk rotor had 1.1–1.2 times the torque of the brake with a plain rotor (Robert, 2017). The form of the conductor slot's surface is next investigated by Prayoga et al. Compared to other shapes, the conductor disc with a semicircular shape has a maximum torque value (Prayoga et al., 2019). In this study, research will be carried out with variations in the number of slots on a semicircular type of conductor plate. The studies in the research is how the number of slots on a semicircular type conductor plate impacts the ECB's braking torque when using a single magnet.

2.0 METHODOLOGY

2.1 Governing Equation

The resulting torque can be influenced by the size of the magnetic field that arises (Cho, Liu, Lee, et al., 2017). The amount of torque on braking can be calculated through the following equation (Rodrigues et al., 2016):

$$T = \frac{1}{2} \times \sigma \delta \omega \pi r^2 m^2 B_z^2 \left[1 - \left\{ \frac{\left(\frac{r}{a}\right)^2}{\left(1 - \left(\frac{m}{a}\right)^2\right)^2} \right\} \right] \quad (1)$$

Where σ is the electrical conductivity of the disc (S/m), δ = disc thickness (mm), ω = angular velocity (rad/s), r = electromagnetic radius (mm), m = distance between disc axis and magnetic axis position (mm), B_z = magnetic flux density (T), and a = disc radius (mm). In equation 2.8 it can be seen that there are several factors that affect the braking torque on the Eddy Current Brake. The influencing factors include the choice of material on the disc conductor, rotational speed, surface area of the electromagnet, magnetic flux density, disc thickness, and disc radius. The area of the electromagnet can also be interpreted as the area of the active region. The active region is the area on the conductor that is perpendicular to the magnetic face, while the passive region is the area that is affected by the magnetic field around the magnetic face. The size of the active region is influenced by the dimensions of the magnetic face and the surface area of the conductor perpendicular to the magnetic face.

The ECB works according to Faraday's law. When a conductor cuts the magnetic force line, it will produce a loop whose magnitude is proportional to the magnetic field and velocity of the conductor (Satya et al., 2021). Faraday's law equation can be seen in equation (2). According to Lenz's law, the rotating loop will generate a new magnetic

field. As a result, the magnet will provide a drag force on the moving conductor (Satya et al., 2021). Lenz's law equation can be seen in equation (3). Conductivity is also important in ECB design because the eddy current is proportional to the eddy current conductivity shown in equation (4). The interaction between eddy currents and magnetic flux density produces a braking force as in equation (5) so that the braking torque equation can be obtained in equation (6).

$$\nabla \times \vec{E} = - \frac{\partial \vec{B}}{\partial t} \quad (2)$$

$$e = (v \cdot B) \cdot l \quad (3)$$

$$\vec{J} = \sigma \cdot \vec{E} \quad (4)$$

$$\vec{F} = \vec{J} \times \vec{B} \quad (5)$$

$$\vec{T} = \vec{F} \cdot r \quad (6)$$

Where \vec{E} = magnetic field intensity (N/C), \vec{B} = magnetic induction (T), e = induced emf (v), v = velocity (m/s), l = conductor length (m), \vec{J} = eddy current density (A/m²), σ = conductivity of the material (S/m), \vec{F} = braking force (N), \vec{T} = torque (Nm), and r = radius (m).

2.2 Developed Model

The finite element method (FEM) is used in this study's simulation process. Fusion 360 software was used for modeling, and Ansys Electronics 2018 was used for simulation. Simulation data is displayed in the form of a curve that represents the rotational speed and braking torque generated for each modification. This simulation uses parameters that affect the performance of the ECB, namely by varying the effect of increasing the number of half-circle slots and comparing the data between all simulation results. Variations in the number of half-circle slots used in this study are 6, 8, 10, and 12 slots. As for variations in rotational speed include 150, 300, 450, 600, and 750 rpm.

The speed variation is also taken from low to high speed in order to know the difference in its effect on braking performance. Then the variation in the number of slots of the half-circle type is carried out in order to find out about the difference in the number of slots that will affect the performance of the Eddy Current Brake which will be better. The variation in the number of slots was chosen based on the fact that the more slots with the half-circle type, the better the braking process performance (Razavi & Lampérth, 2006). The difference in distance between slot variations with a difference of 2 slots is used to find out more details and specifically regarding changes in the addition of braking torque generated in the simulation. The speed variation used refers to the average speed of the vehicle in general. Figure 1 shows the design that will be used in the simulation.

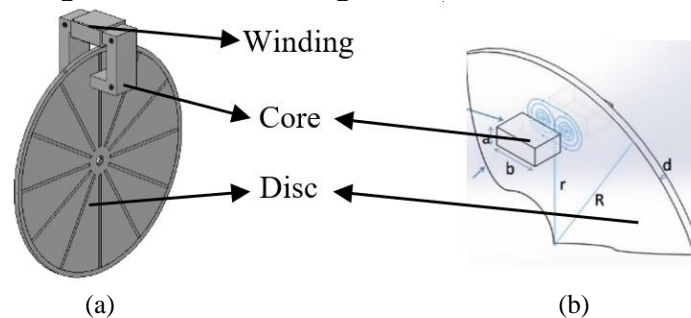


Figure 1. (a) 3D model of a unipolar axial ECB, (b) Eddy current design variable (Waloyo et al., 2020).

Table 1 lists the parameters that were employed in this study's simulation design.

Tabel 1. Design Parameter of ECB (Mufti Reza Aulia Putra et al., 2020).

Variable	Value	Unit
Current (I)	20	A
Count of coil (N)	360	-
Length of pole shoe (a)	30	mm
Wide of pole shoe (b)	12.5	mm
Total length of winding core (l)	248	mm
Distance from center to center of pole shoe (r)	83.5	mm
Air gap	0.5	mm
Thick of disc (d)	5	mm
Radius disc brake (R)	120	mm
Relative permeability aluminium (μ_{al})	1.26×10^{-6}	$H \cdot m^{-1}$
Relative permeability iron (μ_{fe})	6.3×10^{-3}	$H \cdot m^{-1}$
Aluminium conductivity (σ)	36.9×10^6	$S \cdot m^{-1}$

Disc modeling consists of 3 layers, namely disc groove layer, mid layer, and flat layer. Where the groove layer is a layer that is given a half-circle slot, while the flat layer is a layer that is not given a slot. The material used on the disc consists of 2 materials, namely iron material for the mid section and aluminum material for the flat disc section and disc groove (Ubaidillah et al., 2020). The disc parts used can be seen in Figure 2a and the dimensions of the half-circle slots are shown in Figure 2b, where a = thickness, b = slot width, and c = slot depth.

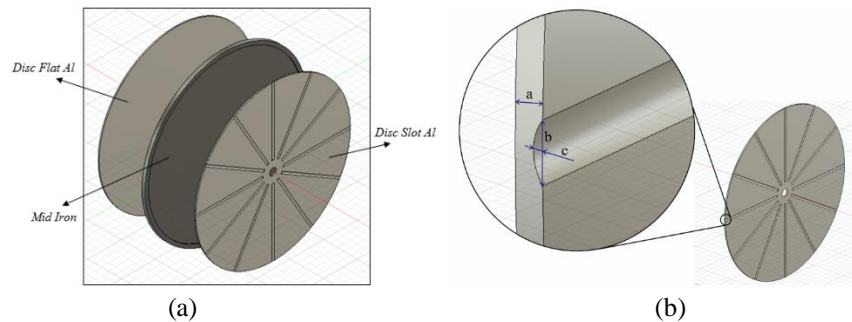


Figure 2. (a) ECB disc section, (b) Aluminum disc slot dimensions.

The meshing used in this study uses a meshing size of 5 mm and the meshing shape is used with a tetrahedral model (M. R.A. Putra et al., 2019). Figure 3 shows an image of the meshing process in the simulation. The materials used in this simulation include aluminum, iron, copper, and air (vacuum). The value of the material properties of these materials is shown in Table 2.

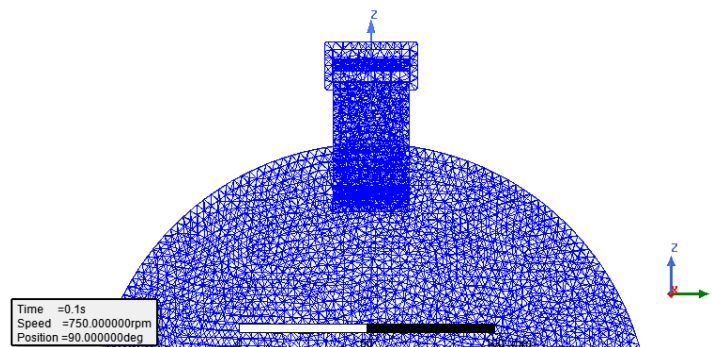


Figure 3. The meshing process in the ECB simulation

Tabel 2. Material Properties

Materials	Relative Permeability (μ_r)	Bulk Conductivity (S/m)	Mass Density (kg/m ³)
Aluminium	1.000021	3.8×10^7	2689
Iron	4000	1.03×10^7	7870
Copper	0.999991	5.8×10^7	8933
Vacuum	1	0	0

3.0 RESULT AND DISCUSSION

3.1 Verification

Data validation was carried out by re-modelling in accordance with the modeling and simulation of previous research. The validation was carried out by comparing the data to the previous research conducted by Putra (M. R.A. Putra et al., 2019). The goal of this simulation is to determine the braking torque and initial flux. Modeling is done by creating a 3D design using Fusion 360 software. The modeling that will be used for data validation is designed as closely as possible to the design to be compared, so that it can produce an assessment similar to the previous design. Validation will hold the simulation's parameters accountability. Table 3 shows a table of data validation against previous studies.

Table 3. Table of data validation against previous research

Rotating Speed (rpm)	Braking Torque (Nm)		Deviation	
	Putra's Research (M. R.A. Putra et al., 2019)	New Research	(%)	%
150	5.086	4.847	4.7	4.7
300	8.300	7.937	4.37	4.37
450	9.429	9.120	3.28	3.28
600	9.383	9.129	2.71	2.71
750	8.828	8.542	3.24	3.24
Average			3.66	

Table 3 shows that the average deviation in this study is 3.66%. This shows that the results of the comparison of data between previous studies and new studies have a deviation of less than 5%. It can be said that the modeling and simulation results are valid.

3.2 Braking Torque

The simulation results for each variation are shown in Table 4.

Table 4. ECB simulation result data

NO	Rotating Speed (rpm)	Braking Torque (Nm)			
		6 Slots	8 Slots	10 Slots	12 Slots
1	150	8.86	8.99	9.18	9.02
2	300	14.09	14.27	14.51	14.26
3	450	15.52	15.71	15.93	15.72
4	600	14.93	15.12	15.30	15.07
5	750	13.66	13.70	13.80	13.63

It can be seen that the largest braking torque in each variation of the number of slots is found at a rotational speed of 450 rpm and the smallest braking torque in each variation is found at a rotational speed of 150 rpm. The highest braking torque value produced is the number of slots 10 with a speed of 450 rpm of 15.93 Nm. After the speed passes 450 rpm, the resulting data will tend to decrease as the rotational speed increases. This is in accordance with the nature and characteristics of the disc conductor used from non-ferrous material, namely aluminum which causes the emergence of critical speed during the braking process (Kou et al., 2014).

Figure 4 shows the relationship between braking torque and rotational speed. The graph shows that each variation in the number of slots has almost the same graphic pattern. Figure 4 shows that when the number of slots increases from 6 to 8 to 10, the brake torque value increases. However, when 12 slots are added to the conductor plate, the value of brake torque produced in 12 slots is less than the value in 10 slots. The chart tends to show a downward trend after crossing the 450-rpm mark. This occurs as a result of the skin effect (Waloyo et al., 2020). Skin effect is an alternating electric current that appears in the disc conductor so that the current density is formed on the surface of the conductor and will decrease as it gets deeper in the conductor (Taghizadeh Kakhki et al., 2016). With the skin effect on the disc conductor, it will greatly affect the braking torque at high speeds (Waloyo et al., 2020). The addition of a semicircular type conductor disc slot on the ECB braking system has only a small impact on the braking performance of the ECB.

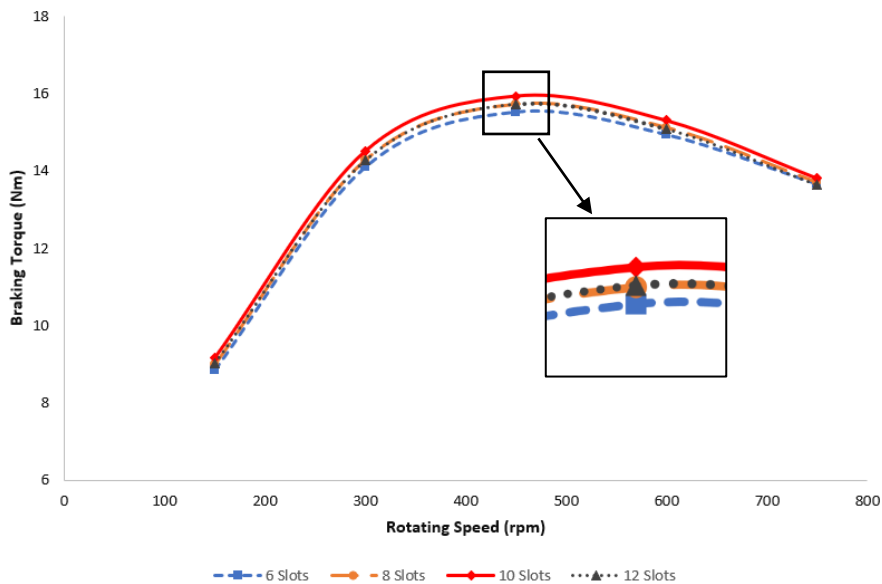


Figure 4. Graph of the relationship between braking torque and rotational speed for each variation

Calculation of braking is done by braking force when the vehicle slows down from a certain speed. The calculation is only to prove the characteristics of the modeling process used, namely regarding the effect of adding a conductor disk slot. At the next stage the braking process can be analyzed with several additional parameters such as rolling resistance, etc.

3.3 Comparison of Magnetic Flux on Variation of Slots

The spread of magnetic flux in each slot variation is shown in Figure 5 below.

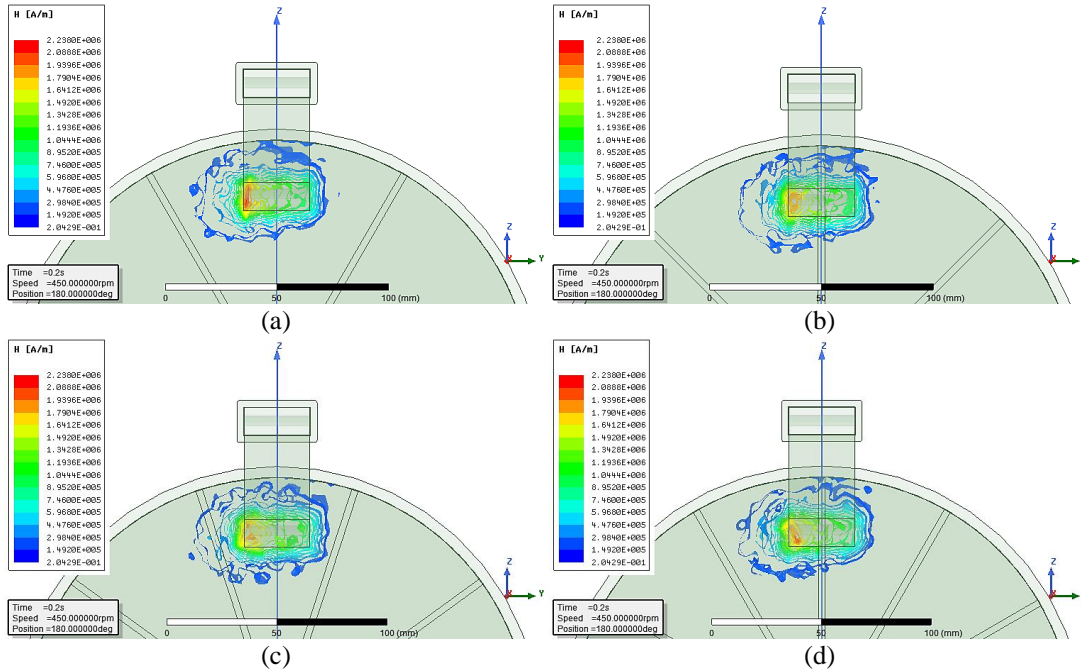
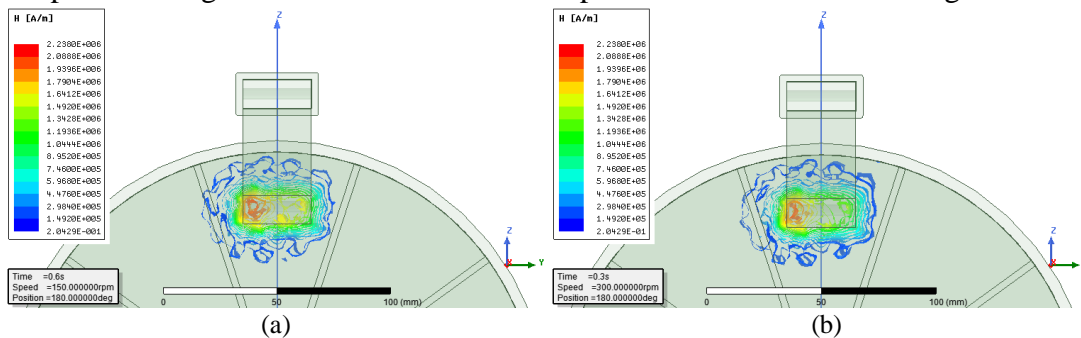


Figure 5. Distribution of magnetic flux in variations of (a) 6 slots, (b) 8 slots, (c) 10 Slots, and (d) 12 slots.

The magnetic flux distribution in Figure 5 in each variation has a magnetic flux distribution that is almost the same or uniform. This makes the addition of the number of half-circle type slots have a less significant effect. The value of the torque produced will also have almost the same value. In addition, the distribution of the magnetic flux is all concentrated in the conductors and cores of the ECB. This phenomenon can be seen in the image in red which indicates that the magnetic field strength is highest in the area closer to the core that carries the electric current.

3.4 Comparison of Magnetic Flux on Rotating Speed

The spread of magnetic flux at each rotational speed variation is shown in Figure 6 below.



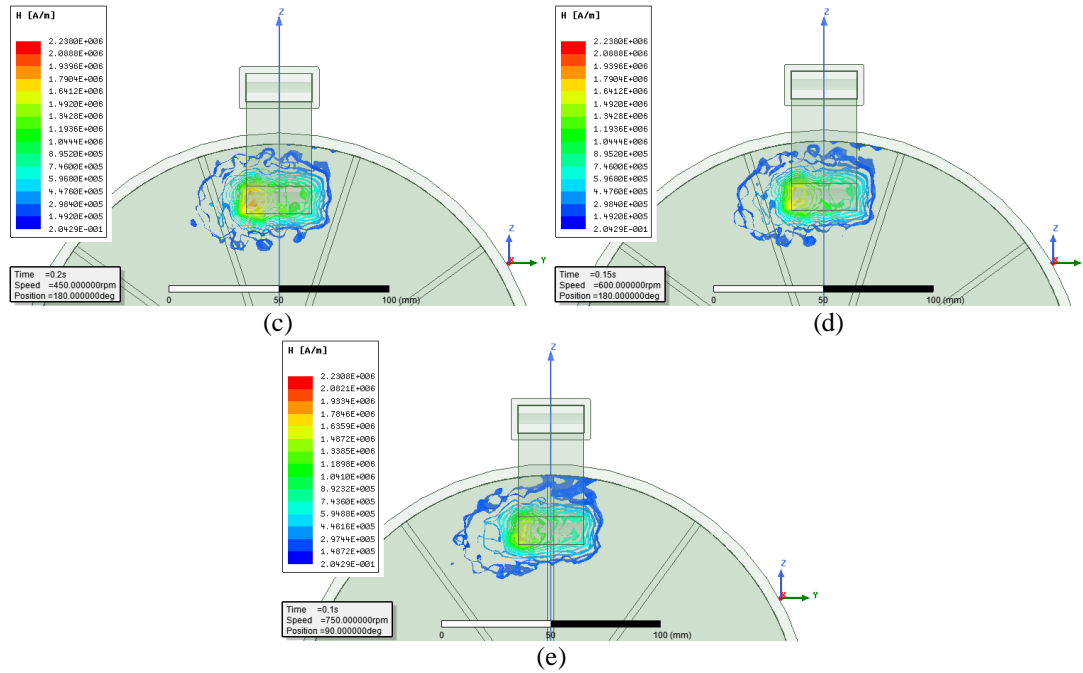


Figure 6. Spread of magnetic flux at variations in rotational speed (a) 150 rpm, (b) 300 rpm, (c) 450 rpm, (d) 600 rpm, and (e) 750 rpm.

In Figure 6 it can be seen that the higher the rotational speed, the greater the spread of the magnetic flux on the disc conductor. In addition, the magnetic field at low speeds is more concentrated to the magnetic source (core) and will spread as the speed increases. The magnetic field strength (red color) will disappear with increasing speed. The phenomenon that occurs is related to the skin effect. The skin effect has a significant impact on braking torque and disc rotation speed (Waloyo et al., 2020). Skin effects appear at high rotational speeds which will cause a decrease in the value of the resulting torque. At low speeds, it is seen that the spread of magnetic flux is still around the center of the magnetic field, while at high speeds the distribution of the magnetic field will be further away from the center of the magnetic field and the resulting area will be larger.

4.0 CONCLUSION

From the research that has been done, it can be concluded that the addition of the number of half-circle type slots with slot variations of 6, 8, 10, and 12 slots does not have a significant effect on the torque generated from the simulation. The trend of the graph of adding slots to the conductor has almost the same trend. The highest braking torque value is produced by a variation of 10 slots with a torque value of 15.93 at a speed of 450 rpm. The spread of magnetic flux in the variation of the number of slots has almost the same area shape. It is concluded that the distribution of magnetic flux with variations in the number of slots does not have much effect on ECB braking. In variations in rotational speed, the spread of magnetic flux from low to high-speed changes the shape of the area. The higher the rotational speed, the wider the magnetic flux distribution because the magnetic field strength will spread and be influenced by the skin effect that appears at high speeds.

5.0 ACKNOWLEDGMENT

Thanks to UNS for providing funding and laboratory facilities for ECB research. Thank you to ICE-SEAM 2021 for accepting and presenting the results of this research work.

6.0 REFERENCES

- Cho, S., Liu, H. C., Ahn, H., Lee, J., & Lee, H. W. (2017). Eddy Current Brake with a Two-Layer Structure: Calculation and Characterization of Braking Performance. *IEEE Transactions on Magnetics*, 53(11). <https://doi.org/10.1109/TMAG.2017.2707555>
- Cho, S., Liu, H. C., Lee, J., Lee, C. M., Go, S. C., Ham, S. H., Woo, J. H., & Lee, H. W. (2017). Design and analysis of the eddy current brake with the winding change. *Journal of Magnetics*, 22(1), 23–28. <https://doi.org/10.4283/JMAG.2017.22.1.023>
- Gerdes, J. C., & Hedrick, J. K. (1999). Brake system modeling for simulation and control. *Journal of Dynamic Systems, Measurement and Control, Transactions of the ASME*, 121(3), 296–503. <https://doi.org/10.1115/1.2802501>
- Günay, M., Korkmaz, M. E., & Özmen, R. (2020). An investigation on braking systems used in railway vehicles. *Engineering Science and Technology, an International Journal*, 23(2), 421–431. <https://doi.org/10.1016/j.jestch.2020.01.009>
- Karakoc, K., Suleman, A., & Park, E. J. (2016). Analytical modeling of eddy current brakes with the application of time varying magnetic fields. *Applied Mathematical Modelling*, 40(2), 1168–1179. <https://doi.org/10.1016/j.apm.2015.07.006>
- Kou, B., Jin, Y., Zhang, H., Zhang, L., & Zhang, H. (2014). Modeling and analysis of force characteristics for hybrid excitation linear eddy current brake. *IEEE Transactions on Magnetics*, 50(11). <https://doi.org/10.1109/TMAG.2014.2323334>
- Lequesne, B. (1997). Eddy-current machines with permanent magnets and solid rotors. *IEEE Transactions on Industry Applications*, 33(5), 1289–1294. <https://doi.org/10.1109/28.633808>
- Prayoga, A. R., Ubaidillah, Nizam, M., & Waloyo, H. T. (2019). The Influence of Aluminum Conductor Shape Modification on Eddy-Current Brake Using Finite Element Method. *ICEVT 2019 - Proceeding: 6th International Conference on Electric Vehicular Technology 2019*, 146–150. <https://doi.org/10.1109/ICEVT48285.2019.8994005>
- Putra, M. R.A., Nizam, M., Tjahjana, D. D. D. P., & Waloyo, H. T. (2019). The Effect of Air Gap on Braking Performance of Eddy Current Brakes on Electric Vehicle Braking System. *ICEVT 2019 - Proceeding: 6th International Conference on Electric Vehicular Technology 2019*, 355–358. <https://doi.org/10.1109/ICEVT48285.2019.8993987>

- Putra, Mufti Reza Aulia, Nizam, M., Tjahjana, D. D. D. P., Aziz, M., & Prabowo, A. R. (2020). Application of multiple unipolar axial eddy current brakes for lightweight electric vehicle braking. *Applied Sciences (Switzerland)*, 10(13). <https://doi.org/10.3390/app10134659>
- Razavi, H. K., & Lampérth, M. U. (2006). Eddy-current coupling with slotted conductor disk. *IEEE Transactions on Magnetics*, 42(3), 405–410. <https://doi.org/10.1109/TMAG.2005.862762>
- Robert, R. S. (2017). 2D model of axial-flux eddy current brakes with slotted conductive disk rotor. *2017 International Siberian Conference on Control and Communications, SIBCON 2017 - Proceedings*, 0–5. <https://doi.org/10.1109/SIBCON.2017.7998501>
- Rodrigues, O., Taskar, O., Sawardekar, S., Clemente, H., & Dalvi, G. (2016). Design & Fabrication of Eddy Current Braking System. *International Research Journal of Engineering and Technology*, 03(04), 809–815.
- Satya, P. S., Chandra, P. G. S., & Raghavendra, M. B. (2021). A Study about Eddy Current Brakes. *IJTIIR*, 50–55.
- Sinmaz, A., Gulbahce, M. O., & Kocabas, D. A. (2016). Design and finite element analysis of a radial-flux salient-pole eddy current brake. *ELECO 2015 - 9th International Conference on Electrical and Electronics Engineering*, 1, 590–594. <https://doi.org/10.1109/ELECO.2015.7394612>
- Taghizadeh Kakhki, M., Cros, J., & Viarouge, P. (2016). New Approach for Accurate Prediction of Eddy Current Losses in Laminated Material in the Presence of Skin Effect with 2-D FEA. *IEEE Transactions on Magnetics*, 52(3). <https://doi.org/10.1109/TMAG.2015.2481924>
- Ubaidillah, U., Suwolo, S., Prayoga, A. R., Nizam, M., & Waloyo, H. T. (2020). Magnetic flux distribution and braking torque of a grooved eddy current brake. *2020 2nd International Conference on Computer and Information Sciences, ICCIS 2020*. <https://doi.org/10.1109/ICCIS49240.2020.9257655>
- Waloyo, H. T., Ubaidillah, U., Tjahjana, D. D. D. P., Nizam, M., & Aziz, M. (2020). A novel approach on the unipolar axial type eddy current brake model considering the skin effect. *Energies*, 13(7), 1–15. <https://doi.org/10.3390/en13071561>